EFFECTS OF LAVA FLOWS ON LUNAR CRATER POPULATIONS

GERHARD NEUKUM and PETER HORN*
Max-Planck-Institut für Kernphysik, Heidelberg, F.R.G.

(Received 18 November, 1975)

Abstract. It is shown that endogenic lava flow processes can be identified by their characteristic effects on lunar crater size distributions without necessarily being able to recognise individual flows on the photographs studied. The thickness of lava flows or a series of flows can be estimated from these crater size distribution characteristics. The lava flow histories of the Apollo landing sites 11, 12 and 15 are discussed in detail. The thicknesses of the most recent (3–3.4 × 10^9 years ago) flows there and of the youngest flows in an area in south-west Mare Imbrium (3 × 10^9 years) are found to range between 30 and 60 m. The subsequent flow episodes at the landing sites showing up in the crater size distributions can be related to differences in the radiometric ages of the respective lunar rocks.

1. Introduction

The lunar surface was modified by endogenic processes over hundreds of millions of years as documented in the wide span of Mare basalt ages. Mare lava extrusions occurred between roughly 4 and 3 aeons ago (e.g., Papanastassiou and Wasserburg, 1971; Stettler *et al.*, 1974). At the same time, the Moon was bombarded by meteoroids. Craters formed and were destroyed by subsequent lava flows. The rejuvenated surfaces have been cratered again and new lava flows may have followed. This interaction of lava flows with crater populations had specific effects on the crater size distributions (Hartmann and Wood, 1970). We want here to discuss these effects in detail with application to crater frequency measurements at the Apollo landing sites 11, 12 and 15.

2. Effects of Lava Flows on Crater Size-distributions

Let us assume we have fresh mare surface ('test surface') just formed by lava extrusion at time t_0. From time t_0 on, a crater population will build up on that surface. If nothing happens to this surface but cratering, we shall at any time see an undisturbed crater population with the primary production size-frequency distribution $N \sim D^{\alpha(D)}$ (N = cumulative crater frequency, D = crater diameter) as given in Figure 1 (Neukum *et al.*, 1975a) provided crater overlap and other erosion processes can be neglected. Though $\alpha(D)$ is a weak function of D, it is sufficient to set α = constant for the following model discussion. On the log-log plot, this distribution is a straight line. In Figure 2 the effects of lava flows on such an idealized distribution $N \sim D^{\alpha}$ is shown. We can distinguish three different cases:

(a) *One subsequent lava flow.* At time t_1 the test surface is flooded. Smaller craters are completely covered, larger craters survive. The original size distribution (indicated by a dashed line for the covered smaller craters) is characteristically

* Present address: Institut für Kristallographie und Petrographie, ETH Zürich, Switzerland

The Moon **15** (1976) 205–222.

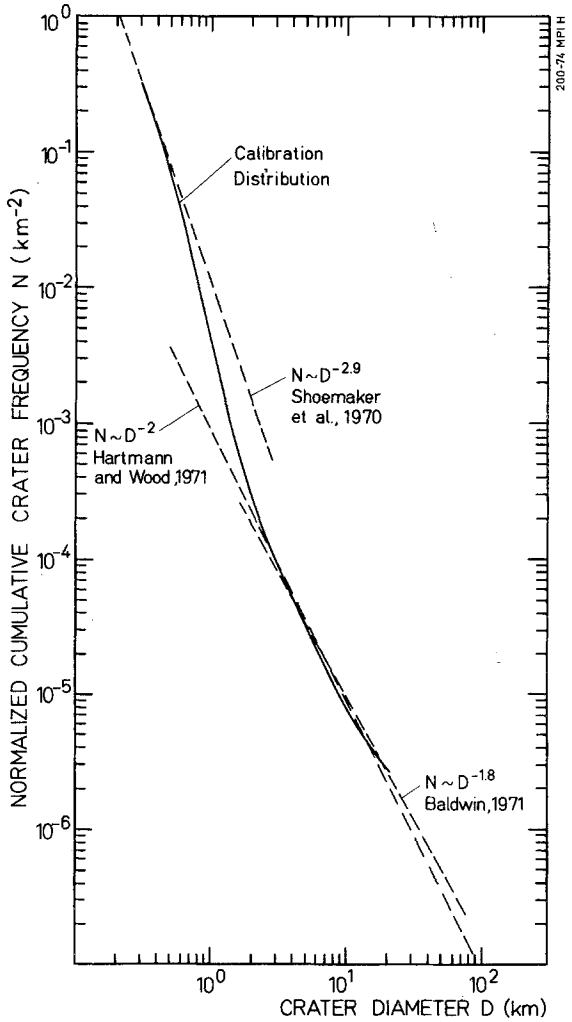

Fig. 1. Lunar crater size-frequency calibration distribution. This curve was derived by Neukum *et al.* (1975a). Every lunar crater size-frequency distribution should follow this standard distribution. Deviations from this curve are indicative of processes (such as lava flows or blanketing by ejecta) affecting and modifying the primary population.

changed. If no additional impacts occur, the post-flooding cumulative crater size distribution is truncated at a certain diameter D_c depending on the thickness of flow, and thus $N = \text{const}$ for smaller sizes. In the time interval between t_1 and t_2, a new post-flooding crater population builds up (t_2 distribution). If no distinction is made, the total crater population observed at time t_2 is the sum of the pre-flooding and the post-flooding population. It is indicated by the thick solid curve. In the size range $D > D_c$, this distribution is parallel to the pre-flooding distribution, though the frequency is higher according to the contribution of the post-flooding population. At $D = D_c$, the distribution flattens abruptly, because the contribution of the pre-

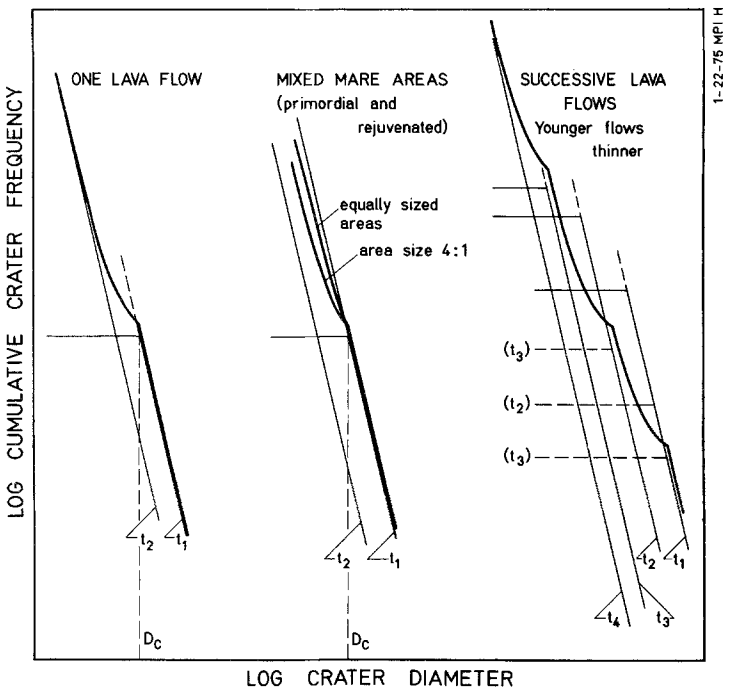

Fig. 2. Effects of subsequent lava flows on an idealized crater size-frequency distribution $N \sim D^{\alpha}$, where α is set constant.

flooding population is zero ($N = \text{const}$). In the size range $D < D_c$, the distribution steepens again and approaches the post-flooding population asymptotically. The irregularity in the size distribution is the greater the smaller the time span $t_2 - t_1$ (that elapsed after the flooding at time t_1) is compared with $t_1 - t_0$ (where t_0 defines the beginning of all cratering on the 'test surface').

(b) *Mixed Mare areas.* It may happen that the 'test surface' is not completely covered by a later lava flow and part of it is not rejuvenated. Let time sequence be the same as in case (a). If no distinction between pre- and post-flooding craters is made in counting, the population observed on the rejuvenated part shows the same irregularity for $D < D_c$ as in case (a). The unaffected population on the non-flooded part of the test area adds to the population of the whole area observed at time t_2. The irregularity (i.e. the 'jump') in the size distribution for $D < D_c$ is obviously less pronounced when the non-flooded area is large compared with the size of the flooded area. As the size of the flooded area dwindles, we should have a 'straight-line' distribution as indicated in Figure 2.

(c) *Successive lava flows.* Lava flows may occur more often. In Figure 2, a special case is shown for successively thinner flows. The test area is thought to be covered completely. The first flow occurs at time t_1. The following post-flooding population is flooded again at time t_2. Craters of the pre-flooding population which survived the flooding at time t_1 will also be affected by the new flows at time t_2. The post-flooding population that has built up in the time span between t_2 and t_3 will be

flooded again at time t_3. Craters of the older populations will also be affected. If the last flow happened at time t_3 and we observed the crater population on the test area at time t_4, we should see the sum of all populations in form of an overall flattened irregular crater size distribution tending to approach the last post-flooding population asymptotically.

In reality, more complex flooding processes may have occurred on the lunar surface, but all effects on crater size distributions should be similar to the discussed three cases or should be composites of it. If flooding occurred only once (case (a) or (b)), the irregularity at crater size $D = D_c$ in the distribution can be used for estimating the flow thickness. According to Pike (1967) the rim height T of a crater of diameter $D < 15$ km reads $T = 0.048\ D^{0.95}$. The flow thickness T_c can thus be calculated for $D = D_c$.

Lava flows are clearly visible in southwest Mare Imbrium on Apollo photographs (Schaber, 1973). The effects of these flows on individual craters can be recognised in detail in some cases. Figure 3a shows an area selected for crater size distribution studies. Figures 3b and 3c show individual craters of this area which have been flooded to various degrees. The lava partly covers only the ejecta blankets or floods

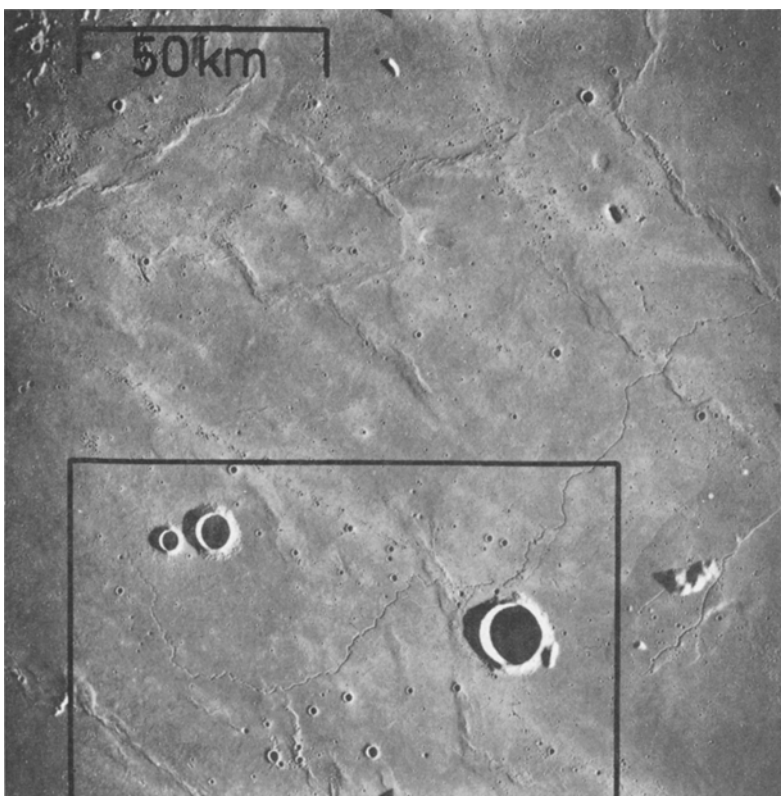

Fig. 3a. Area in Southwest Mare Imbrium (AS17-2929/30; 23°N, 39°W). Lava flows have interacted with the pre-existing crater population.

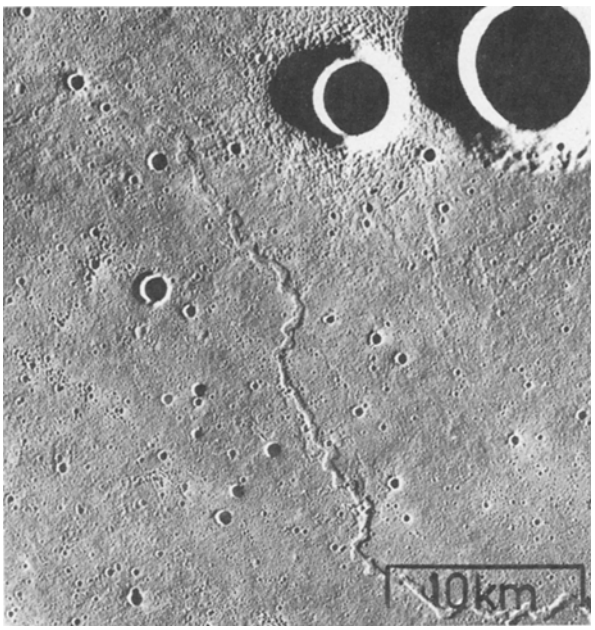

Fig. 3b. Close-up view of examples of craters in this area flooded partly up to their rim crests.

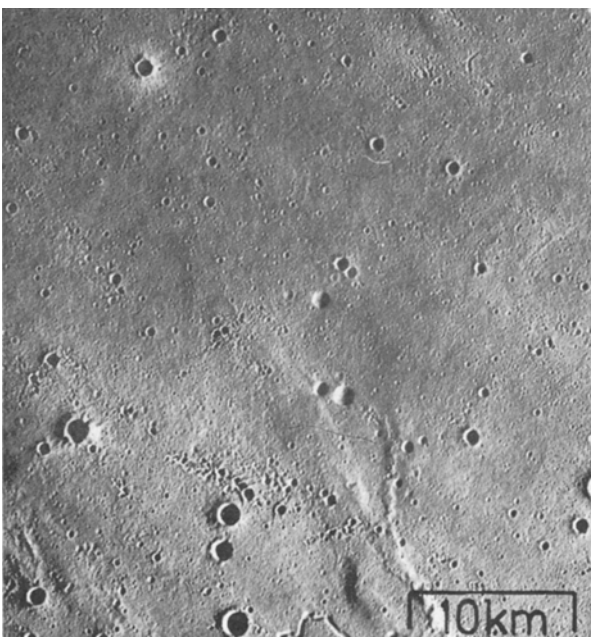

Fig. 3c. Close-up view of craters whose interiors have been flooded or which have been completely covered by lava.

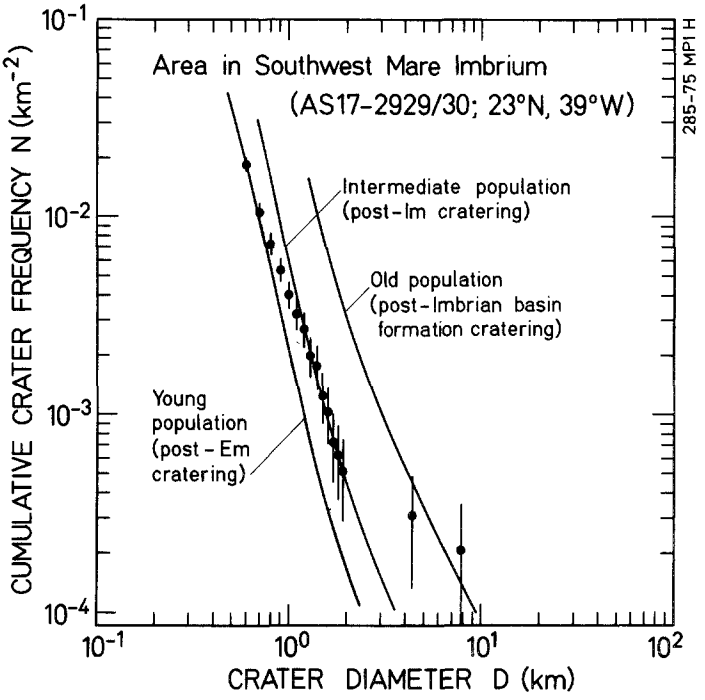

Fig. 4. Crater size-frequency distribution of the area shown in Fig. 3. The subsequent lava flows show up in the irregularities of the distribution (cf. Fig. 2). (Im = Imbrium mare, Em = Eratosthenian mare after Wilhelms and McCauley, 1971)

the craters up to their walls (Figure 3b); in other cases (Figure 3c), craters are covered completely (ghost-craters) or lava flowed over the walls into their interiors.

The crater statistics of this area (Figure 4) show the effects of these lava flows. We can distinguish between three episodes. After the formation of the Imbrium basin (at time t_0 according to the model in Figure 2) a crater population built up ('old population'). It was flooded later (at time t_1). On this fresh mare surface (Imbrium mare = Im) a new crater population built up ('intermediate population'). This population was flooded again later (at time t_2) and a 'young population' of craters built up until today on this Eratosthenian mare (Em) surface. The average total lava flow thicknesses are $T_c \approx 200$ m for the Imbrian mare and $T_c \approx 60$ m for the Eratosthenian mare. The latter value is consistent with Schaber's (1973) data.

The age of these two major flow occurrences can be determined from the crater frequencies according to Neukum *et al.* (1975b). The time for the Imbrian mare filling is determined from the 'intermediate population': $t_1 \approx 3.6 \times 10^9$ years. The Eratosthenian mare filling took place at $t_2 \approx 3.0 \times 10^9$ years. The Em filling may be even slightly younger since we deal with 'mixed mare areas' (Figure 2), though the post-Em cratering is dominant (most of the area investigated is covered by Em flows). A better determination of the age of the youngest flows by counting smaller craters is impossible because of secondary craters stemming from crater Aristarchus (cf. Figure 3).

3. Rock Ages and Crater Populations at the Apollo Landing Sites 11, 12 and 15

Age differences measured for mare basalts from the various landing sites are far greater than the experimental uncertainties which typically lie around 50 m.y. These age differences are attributed to long-lasting eruptive activity at or near the individual localities. Subsequent lava flows were thereby deposited as demonstrated, e.g. by the individual flow units outcropping in the wall of Hadley Rille. As discussed before, the observed age differences between individual flows should show up in the crater size distributions.

3.1. Apollo 11 landing site

Stettler *et al.* (1974) have reported ages for Apollo 11 mare basalts that range between 3.5 and 3.9 b.y. They confirmed and substantiated earlier results by Turner (1970) who already pointed out that chemical differences exist between these rocks (high-K and low-K rocks, respectively). Stettler *et al.* recognize three different age groups which seem to be correlated with petrographical type (Warner, 1971). In addition, Eberhardt *et al.* (1970) found different irradiation histories for members of the high-K and low-K mare basalt groups.

From varying initial Sr isotope ratios for Apollo 11 basalts, three distinct magmatic reservoirs are inferred (Papanastassiou and Wasserburg, 1975). El Goresy and Ramdohr (1975) found mineralogical evidence that subsolidus reduction occurred in some lunar basalts – which frequently is accompanied by K-deposition. If this kind of metasomatism occurred only locally at Apollo 11 (sub-) sites an appreciable time after basalt extrusion – it would be impossible to distinguish it from primary (depositional) age differences under certain circumstances. However – due in part to the lack of water on the Moon – it is unlikely that the metasomatic over-printing

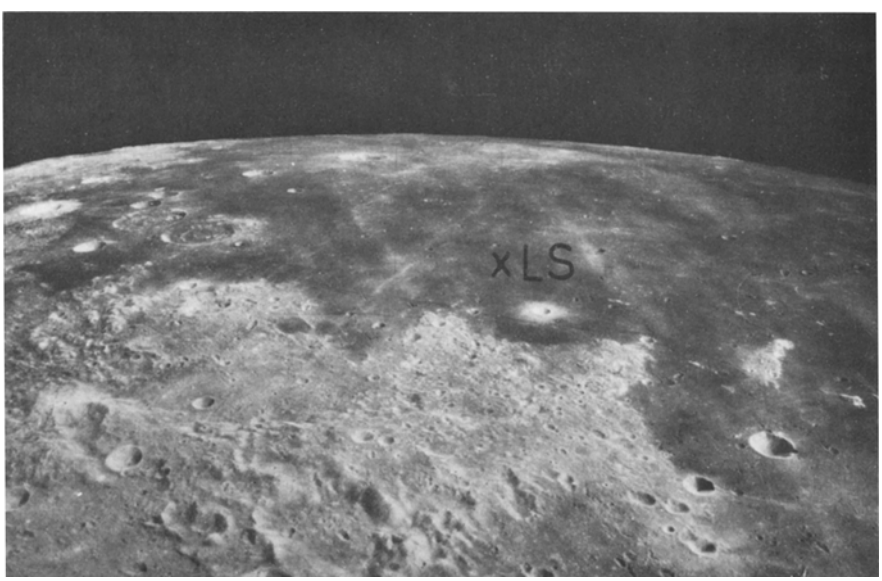

Fig. 5. Surroundings of the Apollo 11 landing site (LS) (16 M 1390 north oblique).

occurred in all mineral phases to the same extent. Hence we agree with Turner (1970) and Stettler *et al.* (1974) that, in fact, samples from lava flows have been dated which repeatedly extruded and solidified over a time span of 400 m.y. (cf. Figure 7). We disagree with Papanastassiou and Wasserburg (1975), who suspect that age differences of high-K and low-K Apollo 11 basalts might be the result of Ar losses from high-K samples preferably because the respective ^{39}Ar–^{40}Ar data show that high and low Ar losses occur both on high-K and low-K basalts.

From an oblique view of the Apollo 11 landing site and surroundings (Figure 5) it can be seen that in the vicinity of the landing site the albedos change drastically, indicating different surface material composition and presumably different lava flows.

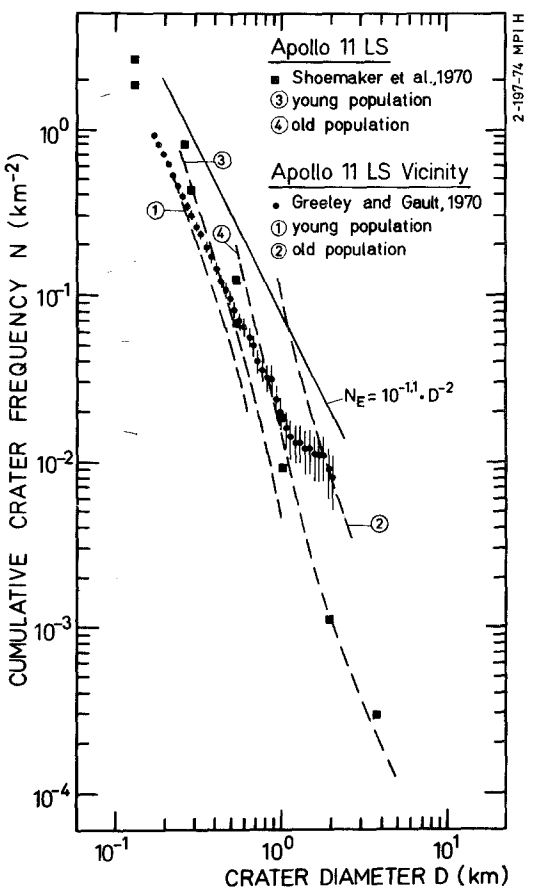

Fig. 6. Crater size-frequency distribution at, and in the vicinity of, the Apollo 11 landing site taken from Shoemaker *et al.* (1970) and Greeley and Gault (1970). These distributions are interpreted to have been affected by subsequent lava flows. This is concluded from the flattening of the measured distributions at smaller sizes compared to the calibration distribution. The frequency of the smaller craters can be associated with the most recent endogenic activities, whereas the larger craters are interpreted to be survivors of the pre-flooding population. The bending over is not due to any crater erosion or superposition effects, because the frequency of the smaller craters is much lower than the equilibrium distribution $N_E = 10^{-1.1} \cdot D^{-2}$ (Trask, 1966).

Crater counts by Shoemaker *et al.* (1970) at the Apollo 11 landing site and those of Greeley and Gault (1970) in its vicinity are shown in Figure 6. Both distributions do not follow the calibration distribution (cf. Figure 1) for smaller crater sizes. The counts of Shoemaker *et al.* show a flattening of the distribution at $D = 0.5$–0.8 km. Unfortunately, these measurements do not allow a more accurate interpretation of the shape of the curve at these small sizes. Greeley and Gault's measurements show an overall depressed size distribution. By comparison with the equilibrium crater size-frequency distribution derived by Trask (1966) it is evident that the flattening of the distributions has nothing to do with crater erosion or superposition effects because the frequencies are far too low. These measurements indicate that at least one lava flow has interacted with the crater population at the Apollo 11 landing site and that several flows have probably occurred in its vicinity. In fact, the size distribution measured by Greeley and Gault resembles very much the case of successive lava flows discussed in Figure 2 (Section 2). The faint changes in slope suggest 3 or more lava flow episodes in the vicinity of the Apollo 11 landing site. These fine breaks in the slope of the distribution are at $D \approx 2$ km, $D \approx 0.9$ km, and $D \approx 0.6$ km.

This finding agrees with the distribution of mare rock ages for the Apollo 11 landing site as discussed above. The radiometric ages as seen in Figure 7 provide us with the onset and termination of a series of flows rather than with the knowledge of distinct episodes; a clustering of ages is, however, indicated for the highest as well as the youngest ages. Thus, it is difficult to associate crater frequencies with ages with much precision. We can, however, approximate by the calibration distribution the lowest crater frequency values found for the smallest craters (curve 1, Figure 6) and tentatively relate this frequency to the lowest rock ages. We assume that these rocks originate from the flows that affected the crater population in the vicinity of the Apollo 11 landing site measured by Greeley and Gault (1970).

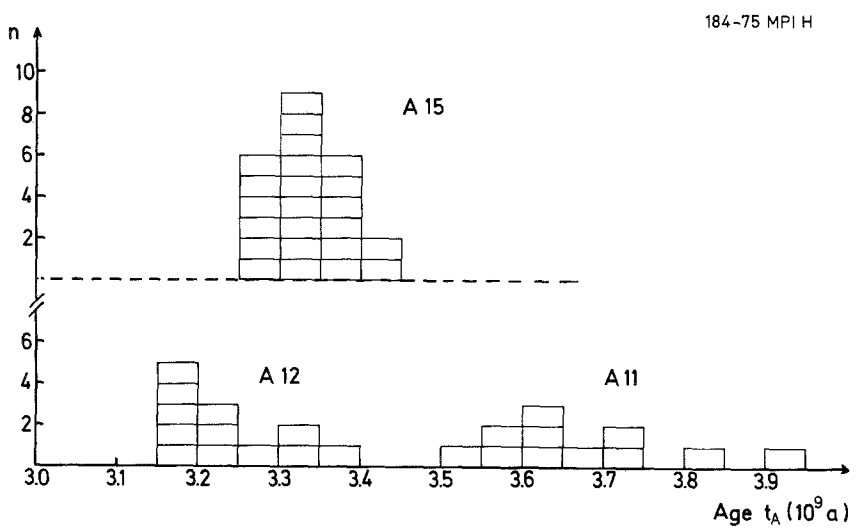

Fig. 7. Histogram of Rb-Sr and K-Ar ages of Apollo 11, 12 and 15 rocks.

Shoemaker *et al.*'s measurements would suggest a somewhat higher frequency for the latest post-flooding population (curve 3 in Figure 6).

Unfortunately, the situation is even less clear for the highest ages. Part of the largest craters must have survived all flows. The frequency of the largest craters in Greeley and Gault's measurements (curve 2 in Figure 6) are too high for any mare surface and indicate ages >4 aeons when comparing with the crater frequencies on the Montes Apenninus or on the Apollo 16 landing site (Neukum *et al.*, 1975b). These craters may be remnants of an ancient highland population that survived flooding. The distance to the Southern Terrae is only about 200 km. The larger craters in Shoemaker *et al.*'s measurements, on the other hand, we regard as being survivors of the population on the oldest mare lavas. This population is approximated by curve 4 in Figure 6. It agrees with the steepening of slope in Greeley and Gault's measurements and the following flattening at $D \approx 0.9$ km which also indicates lava flooding of an ancient mare crater population.

In this way we find two possible associations of crater frequencies with radiometric ages of the Apollo 11 landing site:

(1) Old flows:
Crater frequency for $D = 1$ km: $N \approx 2 \times 10^{-2}$ km^{-2}
Age: $t_A \approx 3.85 \times 10^9$ years

(2) Young flows:
Crater frequency for $D = 1$ km: $N \approx 3.5 \times 10^{-3}$ km^{-2}
Age: $t_A \approx 3.55 \times 10^9$ years.

We want to emphasize that these associations are only tentative ones. The uncertainty in frequency is of the order of a factor of 2. Unfortunately, there does not exist any stereoscopic coverage by Apollo metric or panoramic photography which would probably allow a more detailed investigation.*

3.2. Apollo 12 landing site

The ages measured for Apollo 12 mare basalts range from 3.15 b.y. to 3.36 b.y. (Papanastassiou and Wasserburg, 1971; Turner, 1971; Compston *et al.*, 1971; Horn *et al.*, 1975). The number of rocks dated is rather limited, but as may be seen in Figure 7, a tendency for predominance of rocks having ages around 3.2 b.y. exists.

There are at least 3 different magma generations as pointed out by Marvin *et al.* (1971). Compston *et al.* (1971) recognised a minimum of five chemical groups. Papanastassiou and Wasserburg (1971) observe four different magma sources when considering initial $^{87}Sr/^{86}Sr$-ratios. A straightforward correlation between these parameters and ages does not exist. In general, however, the olivine normative basalts seem to group around 3.3 b.y., while the quartz normative basalts group around 3.2 b.y. and therefore represent the uppermost lava flows there.

The surroundings of the Apollo 12 landing site is shown in Figures 8a and b. In the framed area on Figure 8a and on the whole of Figure 8b, crater counts have been performed by Neukum and König (1976). The counting area in Figure 8a

* There exist stereoscopic Lunar Orbiter coverage of the Apollo 11 landing site. The quality is not known to us. Unfortunately, we have not yet been able to obtain these photographs.

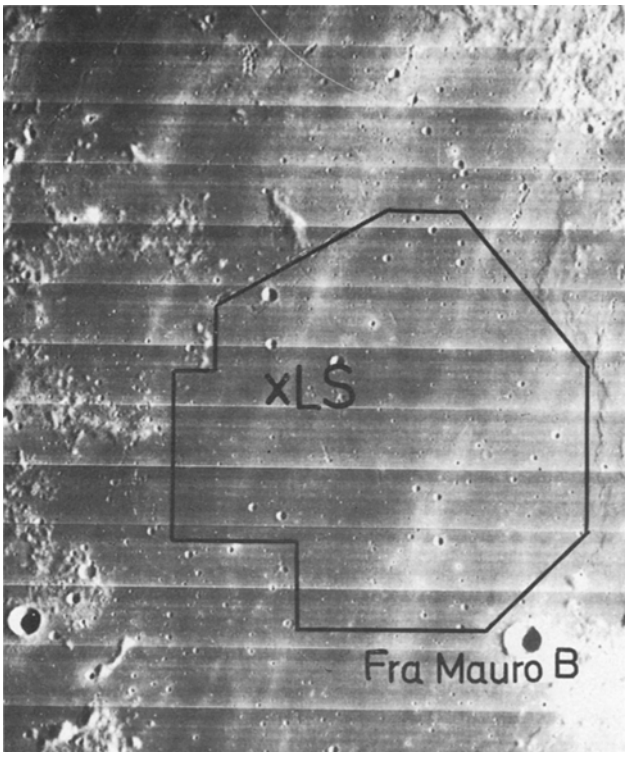

Fig. 8a. Location of the counting area on photograph LO4-125 H3 (Apollo 12 landing site surroundings).

appears to have a somewhat inhomogeneous areal crater distribution with a tendency to show fewer large craters in the immediate surroundings of the landing site and west of it. The resolution of the Lunar Orbiter photograph is too low to identify any lava flow patterns or flow fronts. The immediate surroundings of the landing site (Figure 8b) does not show any clear lava flow pattern either. Stereoscopic high resolution photography of this site does not exist.* We therefore do not know the degree of flooding at the Apollo 12 landing site.

The size frequency measurements in Figure 9, however, tell us that the Apollo 12 landing site region experienced one major subsequent lava flow (or a series of flows in a short time interval) of the type discussed in Section 2(a) and (b). The crater size distribution measured on LO4-125H3 shows a distinct break at $D \approx 1.3$ km. There it flattens abruptly and steepens again at smaller sizes. This indicates a subsequent coverage of the pre-flooding population (curve 2 in Figure 7) by lava with a thickness $T_c \approx 60$ m. As discussed in Section 2, the post-flooding crater population is asymptotically approached by the frequency of the smaller craters. It is approximated in Figure 9 by the calibration curve (curve 1 'young population').

* There exists some stereoscopic medium resolution Lunar Orbiter photography of the Apollo 12 landing site. It has not yet been available to us.

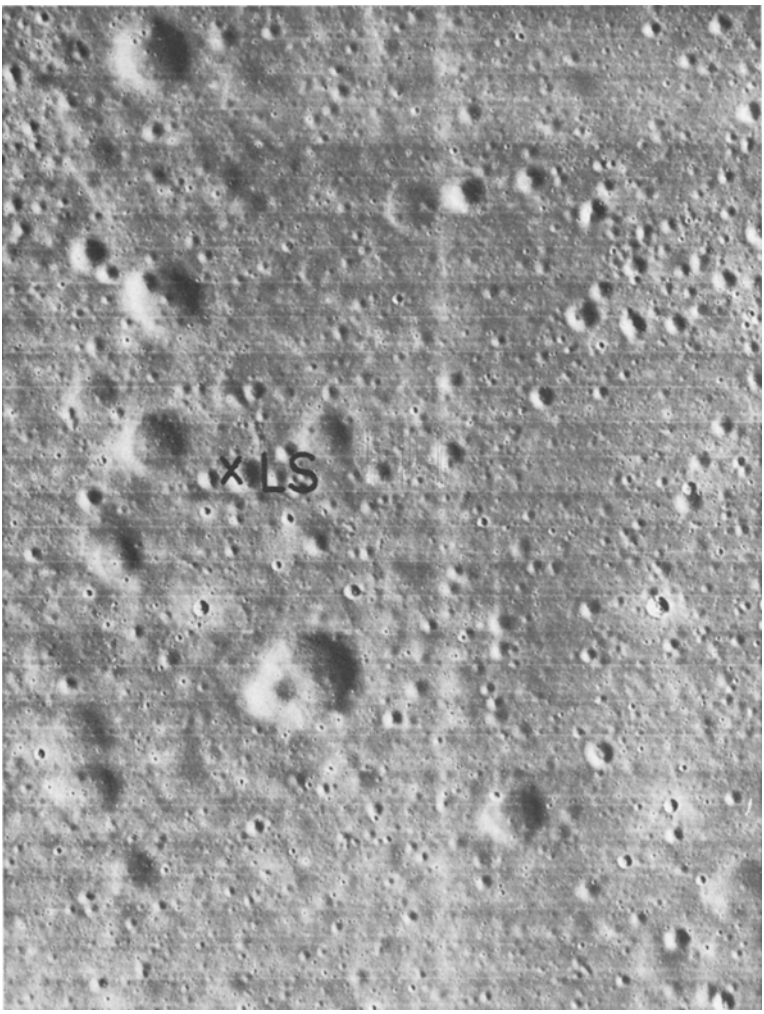

Fig. 8b. Counting area in the immediate surroundings of the Apollo 12 landing site (LO3-154 H2).

This curve also is in rough agreement with the frequency of craters measured in the immediate surroundings of the landing site on picture LO3-154H2. This means that the flooding showing up in the break of the distribution in the farther surroundings of the landing site has also occurred right at the landing site.

We conclude that the population of smaller craters whose frequency is approximated by curve 1 in Figure 9 relates to the uppermost rejuvenated part of the surface. The craters in the immediate surroundings of the landing site have diameters <400 m. Most rocks sampled there have, therefore, been excavated from depths $\ll 80$ m. These must be the rocks grouping around $t_A = 3.2$ aeons in Figure 7. Thus, it is $N \approx 2.5 \times 10^{-3}$ km^{-2} for $D = 1$ km and age $t_A \approx 3.2$ aeons for the Apollo 12 landing site.

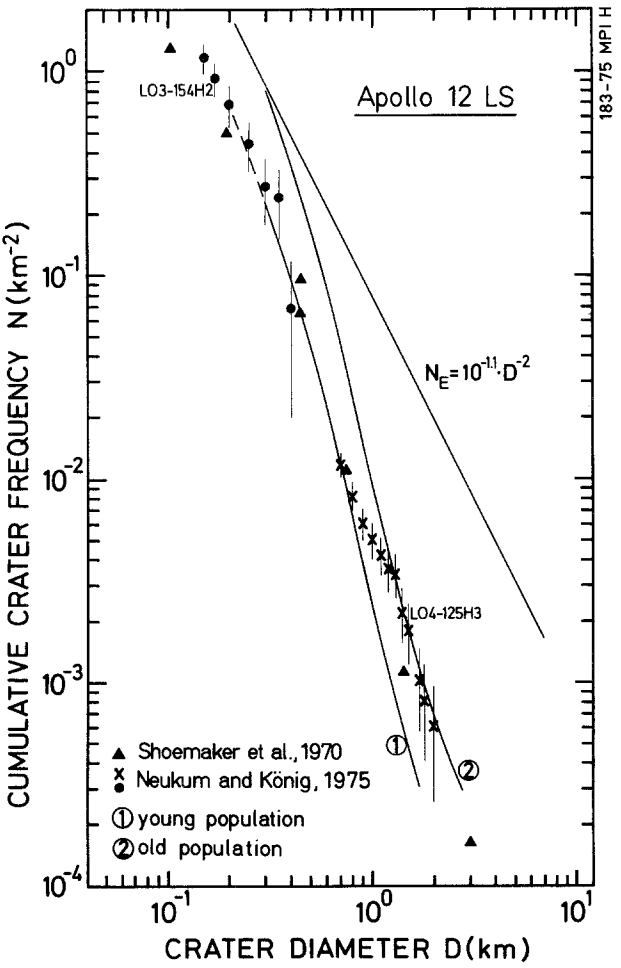

Fig. 9. Crater size-frequency distributions measured at the Apollo 12 landing site (Neukum and König, 1975). The distribution measured on LO4-125 H3 shows a pronounced irregularity at $D \approx 1.3$ km which is indicative of a subsequent lava flow destroying the craters with $D < 1.3$ km. The size-frequency distribution measured in the immediate surroundings of the landing site on LO3-154 H2 gives values compatible with that for the smallest craters from LO4-125 H3 (comparing with the calibration distribution). Earlier measurements by Shoemaker *et al.* (1970) are also shown for comparison.

The occurrence of a few rocks as old as 3.4 aeons agrees with the fact that a few impacts have penetrated to depths >60 m and must have excavated rocks of older mare surfaces. The difference in crater frequency between the 'young population' and the 'old population' in Figure 9, however, suggests an age difference of more than 200 m.y. for the primordial and rejuvenated surface according to Neukum and König (1976) and Neukum *et al.* (1975b). Rocks as old as 3.6 aeons should exist among the Apollo 12 samples. Another possible interpretation of this slight disagreement is that two lava flows happened within a time span of 200 m.y. and the resolution in the crater frequency measurements is not high enough for

recognizing it. The interpretation is further complicated by the fact that a clear distinction between case (a) (complete flooding of the counting area) or case (b) (mixed mare areas) (Figure 2) cannot be made. From the crater statistics, it seems that the greatest part of the accounting area has been affected by the subsequent flooding. This is also supported by the albedo differences in Figure 8a. Only small parts of the original (pre-flooding) surface in the east of the counting area may not have been affected (higher albedo). Unfortunately, the overlain ray system of crater Copernicus renders interpretation of albedo differences difficult.

3.3. APOLLO 15 LANDING SITE

A relatively large number of Apollo 15 mare basalts have been dated with ages between 3.13 b.y. and 3.44 b.y. (Husain, 1974; Papanastassiou and Wasserburg, 1973). The age histogram in Figure 7 shows a pronounced peak around 3.3 b.y. The $^{39}Ar/^{40}Ar$ plateau ages younger than 3.25 b.y. reported by Husain are suspected by us to be lowered by Ar loss on the Moon, since total Ar losses for these samples are very high. They are, therefore, not included in our age histogram. The last lava extrusions in Palus Putredinis of Mare Imbrium occurred in the time interval from 3.4 to 3.25 b.y.

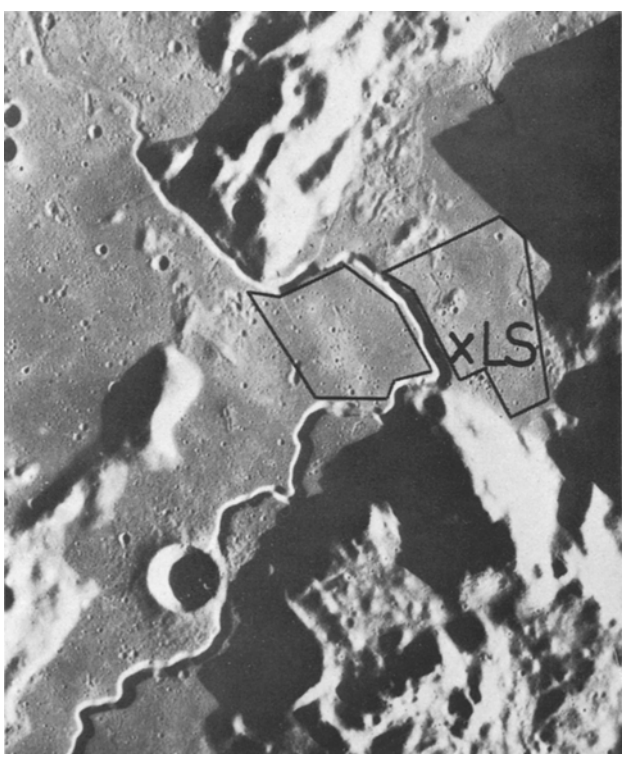

Fig. 10. Location of the counting area at the Apollo 15 landing site (15 M 415).

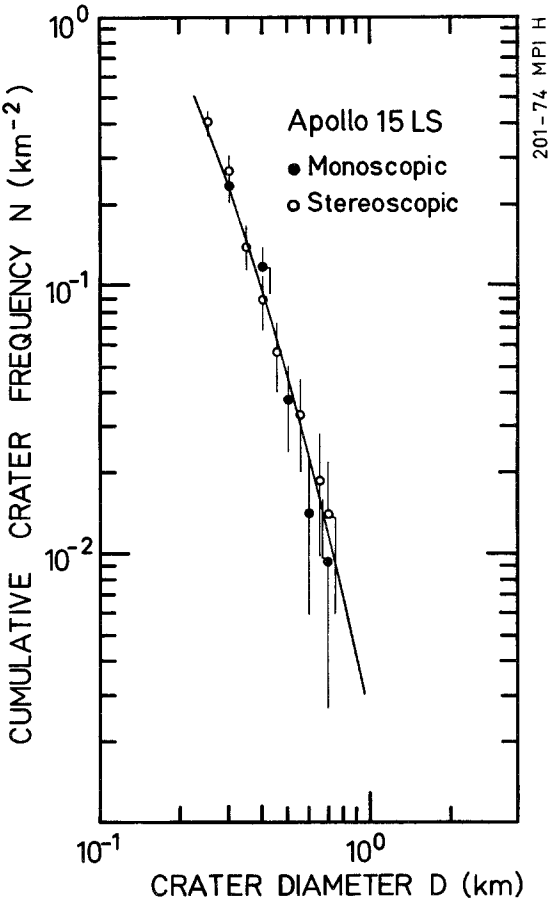

Fig. 11. Crater size-frequency distribution at the Apollo 15 landing site (Neukum *et al.*, 1975a). It is in good agreement with the calibration distribution (solid curve).

A correlation between chemical and mineralogical type and age for Apollo 15 basalts is not evident (Husain, 1974). From initial $^{87}Sr/^{86}Sr$ ratios, Compston *et al.* (1972) concluded that only a single magma source was activated.

Crater counts at the Apollo 15 landing site have been performed by Neukum *et al.* (1975a). The counting area is shown in Figure 10. Both regions have yielded the same crater frequency within the error limits. The total crater size frequency distribution is shown in Figure 11. The good approximation of the measured distribution with the calibration distribution shows that the visible crater population is largely undisturbed by lava flows. There are, however, some larger craters in the counting area which could be survivors of an older crater population mainly lying on a hilly kipuka-like area as indicated in Figure 12. (There are other clusters of mainly smaller craters in this area, especially that in the lower right corner of Figure 12. These are secondary craters probably stemming from crater Autolycus or crater Aristillus.) A ghost crater is to be seen between the

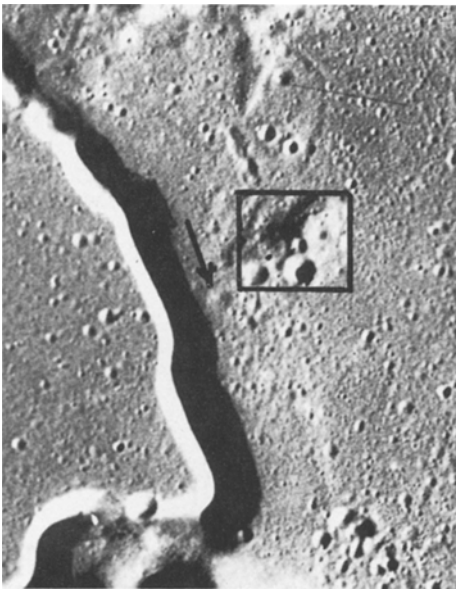

Fig. 12. Close-up view of the Apollo 15 landing site surroundings. A kipuka-like structure is framed. The arrow points towards a ghost-crater right by Hadley Rille.

kipuka-like structure and Hadley Rille (pointed out by the arrow on Figure 12). These observations indicate that the crater population in this area has been influenced by one or more flows but that one of the most recent flows (or a series of flows) must have been very effective and has almost completely rejuvenated the surface. The crater size frequency distribution data are in good agreement with the rock age data. The observed ghost-crater indicates a flow thickness of $T_c \approx 30$ m.

4. Conclusions

The history of the formation of the lunar surface as seen today can only be inferred from a close co-examination of such surface features as crater populations or individual lava flows together with radiometric age information as well as the chemistry and mineralogy of the rocks sampled on the lunar surface. Unfortunately, the surface photography permits an identification of individual lava flows only in a few cases. Besides remote sensing of physical and chemical surface properties, investigations of crater populations in the 100-meter to kilometer size range can shed light on the development of the lunar surface at individual sites. The potential of such investigations performed in this paper is summarized in the following:

(1) Endogenic processes interact with cratering characteristically.

(2) Endogenic processes can be identified by the crater size distribution characteristics without necessarily being able to recognize individual lava flows on the photographs studied.

(3) The thicknesses of lava flows or a series of flows can be estimated from the characteristic deviations in the size frequency distributions of the affected crater populations.

(4) Radiometric age differences can be related to size-frequency differences of crater populations.

We regard these investigations of the Apollo 11, 12 and 15 landing sites as a beginning. Better resolution photography would certainly reveal more details, especially for the Apollo 11 landing site. More radiometric age data are also necessary.

Similar investigations remain to be done for the other mare landing sites, Apollo 17 and Luna 16. The limited areas and the small crater sizes at these sites pose an additional problem however (Neukum and König, 1976). The size-frequency distribution of the 100-meter size range craters is not well enough known, and furthermore only two age determinations exist for Luna 16.

Acknowledgements

This project was supported by the Bundesministerium für Forschung und Technologie and the Deutsche Forschungsgemeinschaft. We thank Dr S. E. Dwornik, Chief of the Office of Space Science, NASA Headquarters, Washington D.C., and Dr J. I. Vette, Director of World Data Center A for Rockets and Satellites, Goddard Space Flight Center, Greenbelt, Maryland, for providing the photographic material for our studies. Assistance and advice by our colleagues of the Cosmochemistry Department of the Max-Planck-Institut für Kernphysik, Heidelberg, is gratefully acknowledged.

References

Compston, W., de Laeter, J. R., and Vernon, M. J.: 1972, In: *The Apollo 15 Lunar Samples*, 347, The Lunar Science Institute, Houston.

Compston, W., Berry, H., Vernon, M. J., Chappell, B. W., and Kaye, M. J.: 1971, Proc. Second Lunar Sci. Conf., *Geochim. Cosmochim. Acta*, Suppl. 2, Vol. 2, 1471, MIT-Press.

Eberhardt, P., Geiss, J., Graf, H., Grögler, N., Krähenbühl, U., Schwaller, H., Schwarzmüller, J., and Stettler, A.: 1970, *Earth Planet. Sci. Lett.* **10**, 67.

El Goresy, A. and Ramdohr, P.: 1975, In: *Lunar Science* **VI** 245, The Lunar Science Institute, Houston.

Greeley, R. and Gault, D. E.: 1970, *The Moon* **2**, 10.

Hartmann, W. K. and Wood, C. A.: 1971, *The Moon* **3**, 3.

Horn, P., Kirsten, T., and Jessberger, E. K.: 1975, *38th Ann. Meet. Met. Soc.*, Tours.

Husain, L.: 1974, *J. Geophys. Res.* **79**, 2588.

Marvin, U. B., Wood, J. A., Taylor, G. J., Reid Jr., J. B., Powell, B. N., Dickey Jr., J. S., and Bowes, J. F.: 1971, Proc. Second Lunar Sci. Conf., *Geochim. Cosmochim. Acta*, Suppl. 2, Vol. 1, 679, MIT-Press.

Neukum, G., and König, B.: 1976, to be published.

Neukum, G., König, B., and Arkani-Hamed, J.: 1975a, *The Moon* **12**, 201.

Neukum, G., König, B., Fechtig, H., and Storzer, D.: 1975b, accepted for publication Proc. Sixth Lunar Sci. Conf.

Papanastassiou, D. A. and Wasserburg, G. J.: 1973, *Earth Planet. Sci. Lett.* **17**, 324.

Papanastassiou, D. A. and Wasserburg, G. J.: 1975, In: *Lunar Sci.* **VI**, 631, The Lunar Science Institute, Houston.

Pike, R. J.: 1967, *J. Geophys. Res.* **72**, 2099.

Schaber, G. G.: 1973, Proc. Fourth Lunar Sci. Conf., Suppl. 4, *Geochim. Cosmochim. Acta*, Vol. 1, 73.

Shoemaker, E. M., Batson, R. M., Bean, A. L., Conrad, C., Jr., Dahlem, D. H., Goddard, E. N., Hait, M. H., Larson, K. B., Schaber, G. G., Schleicher, D. L., Sutton, R. L., Swann, G. A., and Waters, A. C.: 1970, NASA SP-235, 113.

Stettler, A., Eberhardt, P., Geiss, J., Grögler, N., and Maurer, P.: 1974, Proc. Fifth Lunar Sci. Conf., *Geochim. Cosmochim. Acta*, Suppl. 5, Vol. 2, 557, Pergamon.

Trask, N. J.: 1966, 'Size and Spatial Distribution of Craters Estimated from Range Photographs', Jet Propul. Lab. Tech. Rep. 32-700, Pasadena, Calif. p. 252.

Turner, G.: 1970, Proc. Apollo 11 Lunar Sci. Conf., *Geochim. Cosmochim. Acta*, Suppl. 1, Vol. 2, 1665, Pergamon.

Turner, G.: 1971, *Earth Planet. Sci. Lett.* **11**, 169.

Warner, J. L.: 1971, Proc. Second Lunar Sci. Conf., *Geochim. Cosmochim. Acta*, Suppl. 2, Vol. 1, 465, MIT-Press.

Wilhelms, D. E. and McCauley, J. F.: 1971, 'Geologic Map of the Near Side of the Moon', U.S. Geol. Survey Misc. Geol. Inv. Maps I-703.